

## Electronic Supplementary Information

# **A Facile Synthesis of Fe/N-doped Ultrathin Carbon Sheet for Highly Efficient Oxygen Reduction Reaction**

Pingping Zhao, Qiuxiang Mou, Xinghai Liu, Houbin Li, and Gongzhen Cheng

## **Table of contents**

1. Supplementary Figures.....	1
2. Supplementary Tables .....	8
Reference.....	11

## 1. Supplementary Figures

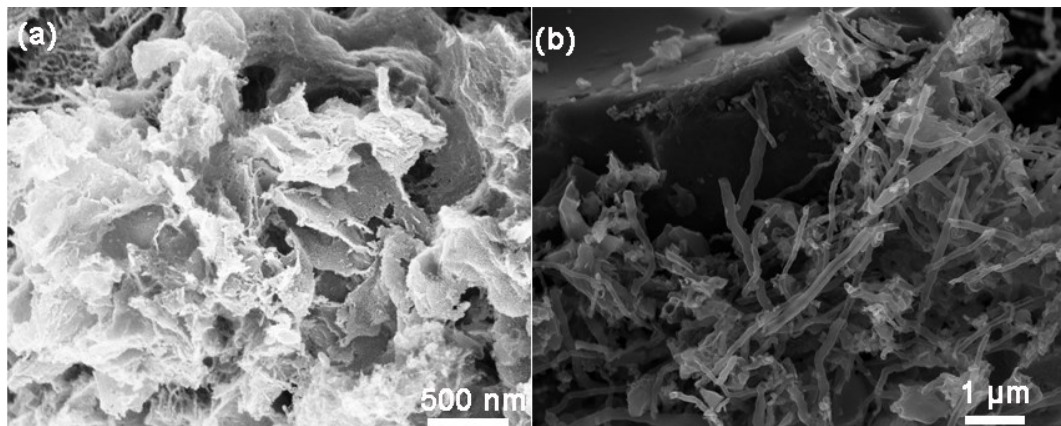


Figure S1. SEM images of the catalysts Fe<sub>3</sub>C/NC-800 and FeNC-800-M.

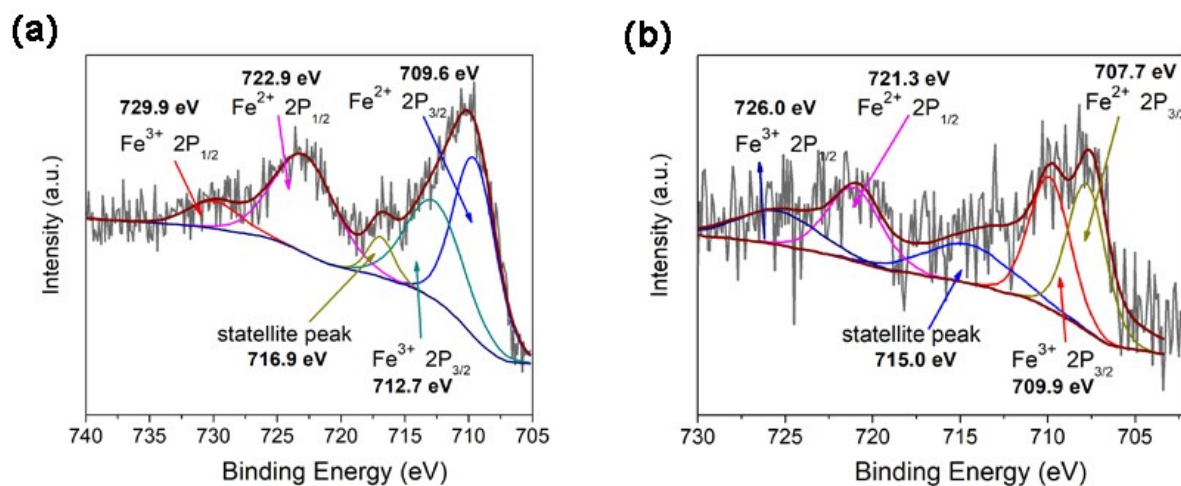


Figure S2. High resolution of Fe 2p of (a) Fe<sub>3</sub>C/NC-800 and (b) FeNC-800-M.

(Fe<sub>3</sub>C/NC-800 exhibited a much larger binding energy than that of FeNC-800-M, and Fe (II) and Fe (III) type with different binding energy can be distinguished. The peak of Fe<sup>3+</sup> 2P<sub>3/2</sub> was considered to be Fe connected to N, the resulting FeN<sub>4</sub> structure is generally recognized as the active sites, especially in alkaline solution.)

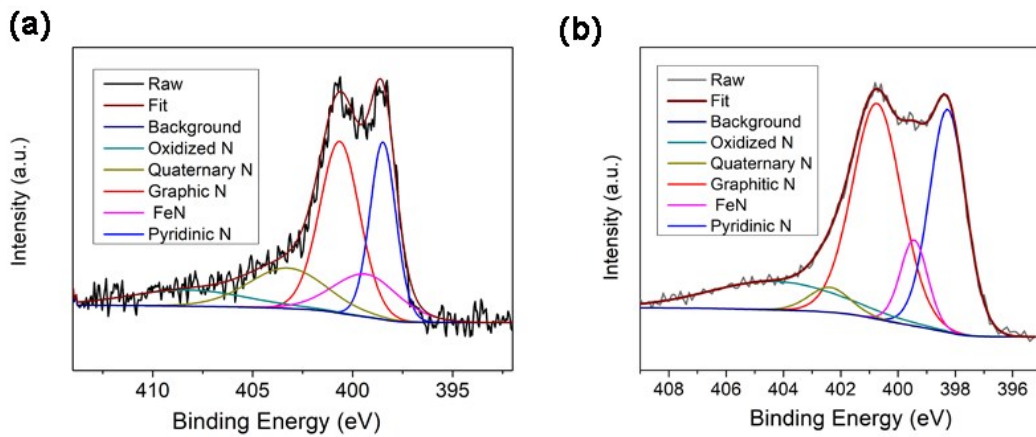


Figure S3. High resolution of N 1s of (a) Fe<sub>3</sub>C/NC-800 and (b) FeNC-800-M.

(The binding energy could be divided into five types: graphitic N, pyridinic N, oxidized N, quaternary N and FeN. In ORR catalytic process, pyridinic N and FeNx was thought to be the major contributor to enhance the electrochemical performance.)

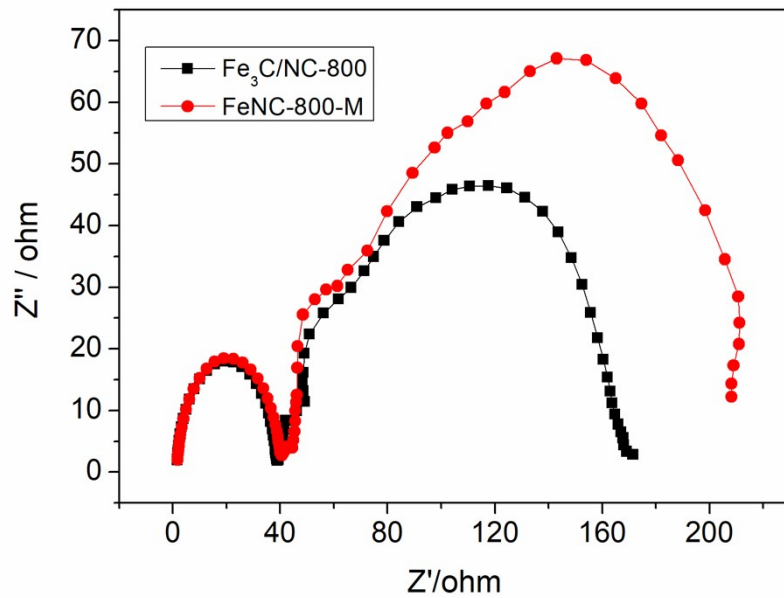


Figure S4. Electrochemical impedance spectroscopy data for FeNC-800-M (red line) and Fe<sub>3</sub>C/NC-800 (black line).

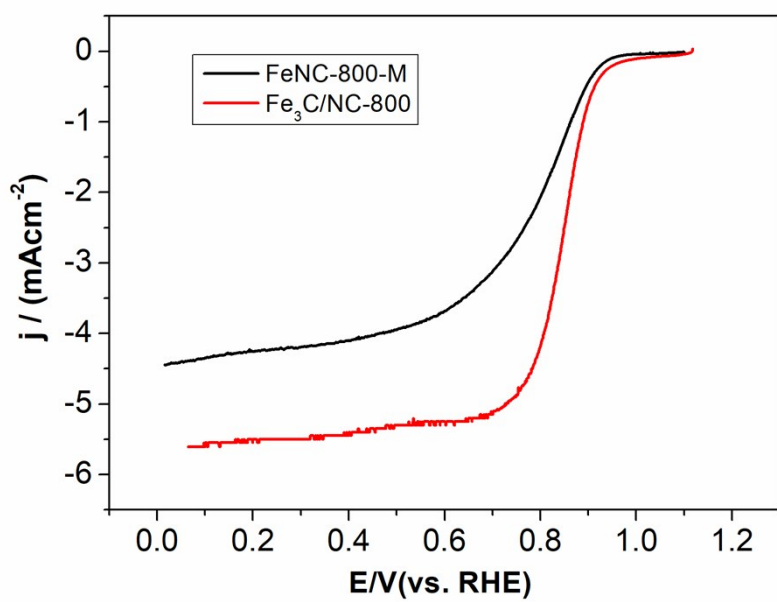


Figure S5. Steady-state polarization curves of ORR for  $\text{Fe}_3\text{C}/\text{NC}-800$  (red line) and FeNC-800-M (black line) in 0.1M KOH solution.

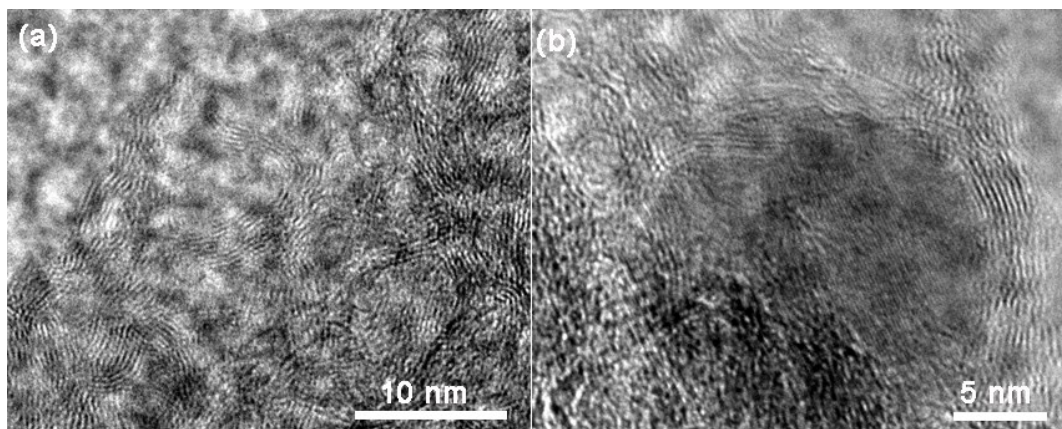


Figure S6. HRTEM images of the catalysts  $\text{Fe}_3\text{C}/\text{NC}-800$ .

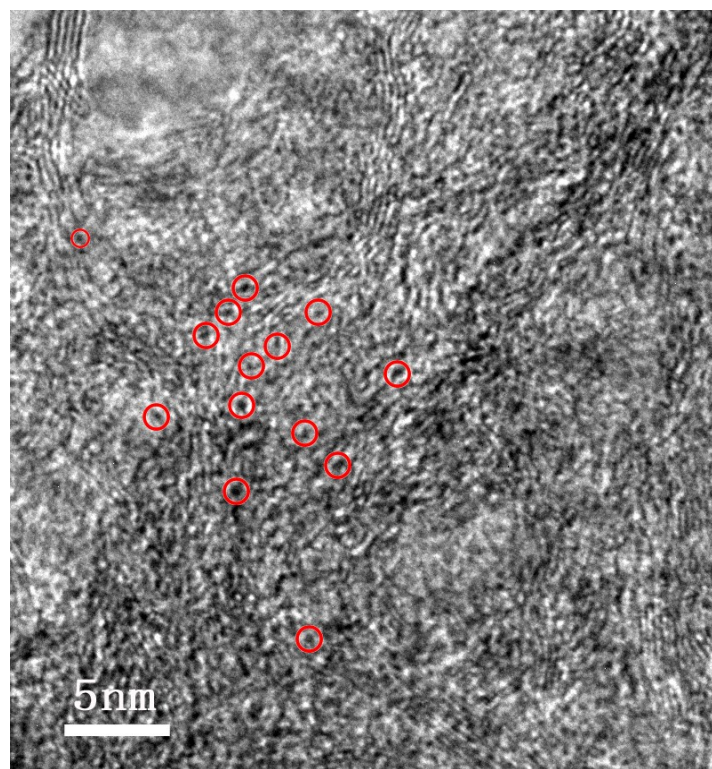


Figure S7. High resolution TEM image of Fe<sub>3</sub>C/NC-800.

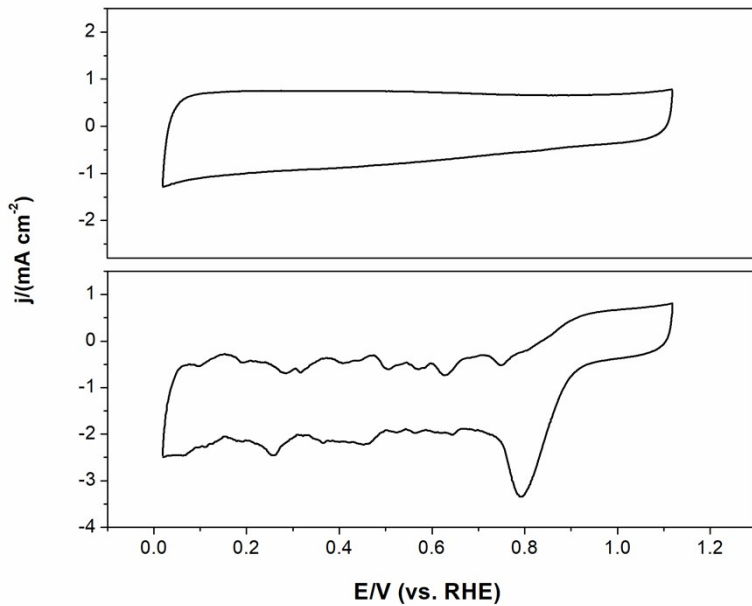


Figure S8. Cyclic voltammograms for Fe<sub>3</sub>C/NC-800 obtained in 0.1 M KOH with Ar (up) and O<sub>2</sub> (down) saturated. The scan was performed negatively.

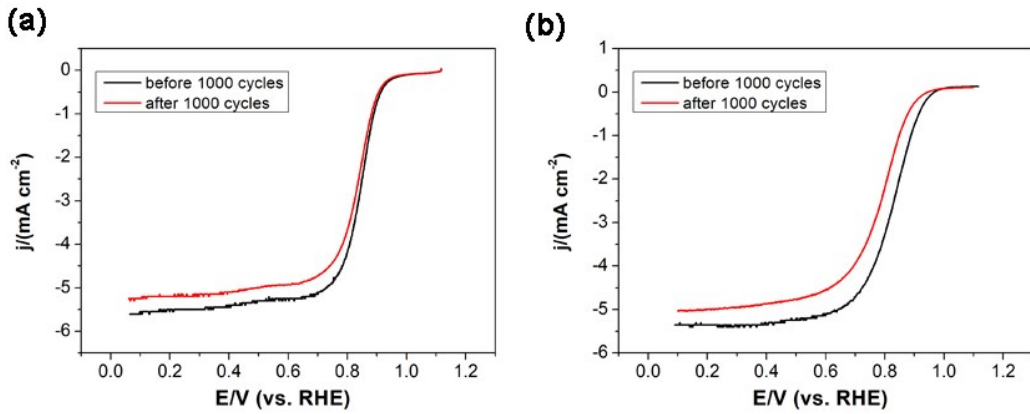


Figure S9. The activities after 1000 cycles of  $\text{Fe}_3\text{C}/\text{NC}-800$  and Pt/C in an  $\text{O}_2$ -saturated 0.1 M KOH solution.

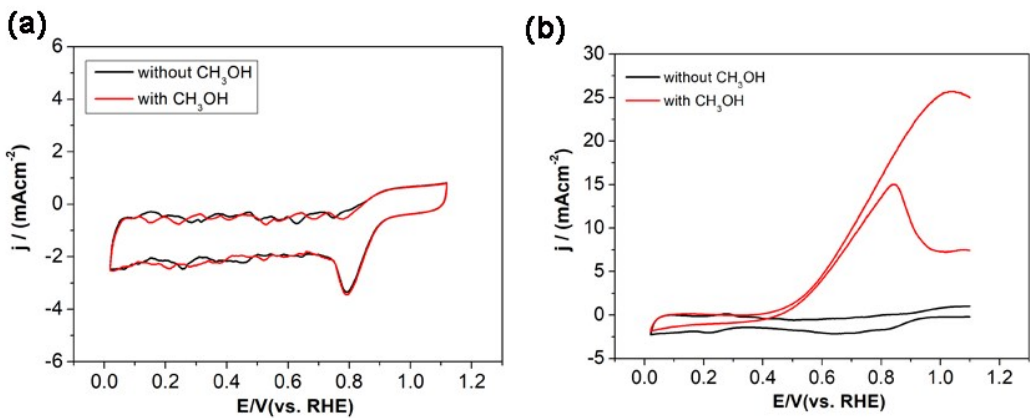


Figure S10. Cyclic voltammograms of (a)  $\text{Fe}_3\text{C}/\text{NC}-800$  and (b) Pt/C in an  $\text{O}_2$ -saturated 0.1 M KOH solution containing 1M methanol. The scan was performed negatively.

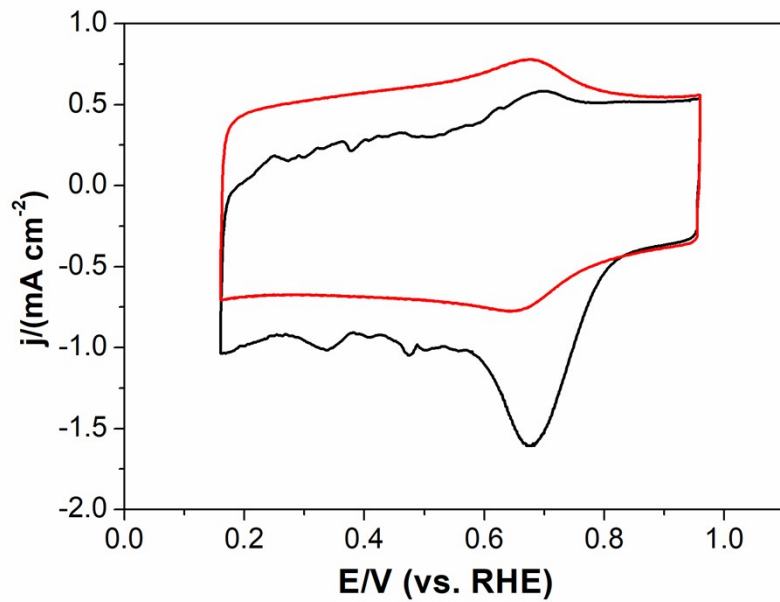


Figure S11. Cyclic voltammograms for  $\text{Fe}_3\text{C}/\text{NC}-800$  obtained in 0.1 M  $\text{HClO}_4$  at a scanning rate of 50 mV/s with  $\text{O}_2$  saturated (black line) and Ar saturated (red line). The scan was performed negatively.

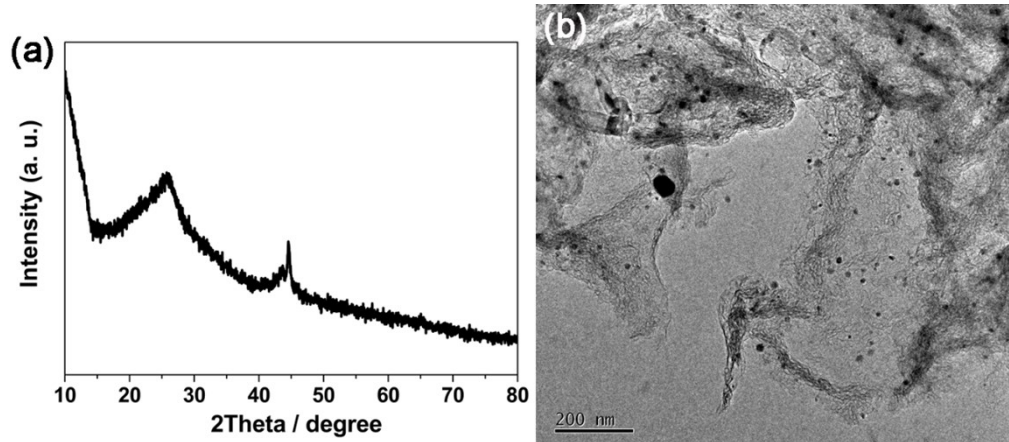


Figure S12.  $\text{Fe}_3\text{C}/\text{NC}-800$  catalyst after  $i-t$  test: (a) XRD pattern; (b) TEM image.

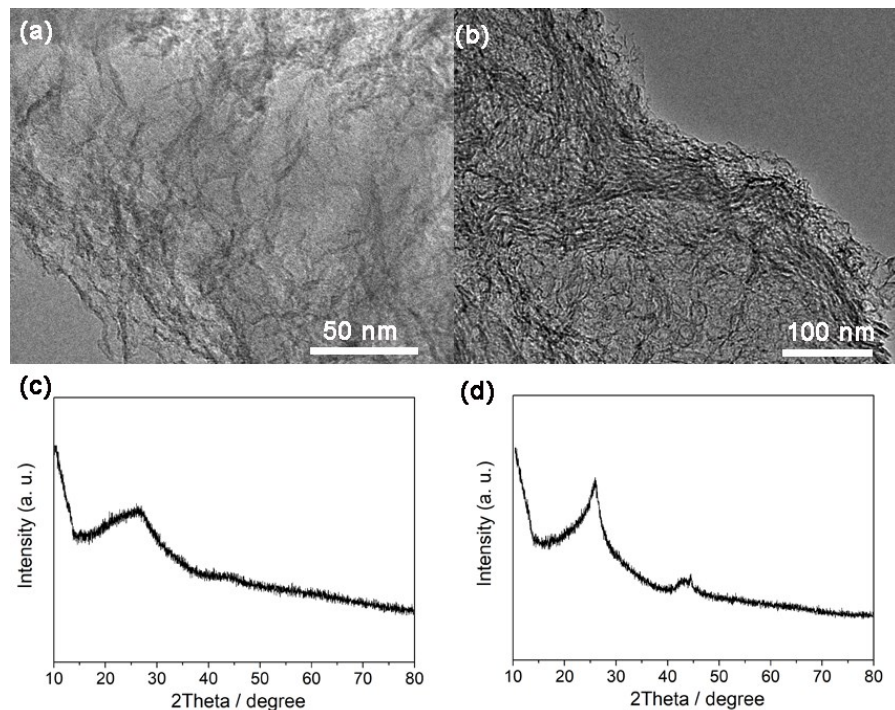


Figure S13. TEM images and XRD patterns of the FeNC-700 (a, c) and FeNC-900 (b, d).

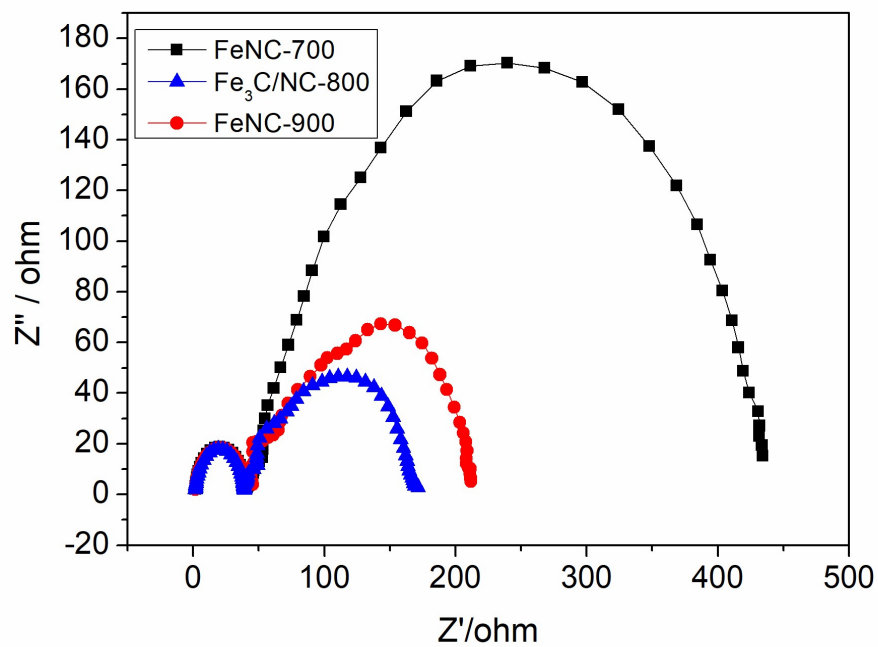


Figure S14. Electrochemical impedance spectroscopy data for samples obtained at 700, 800 and 900 °C, respectively.

## 2. Supplementary Tables

Table S1. Percentage of different kinds of N in  $\text{Fe}_3\text{C}/\text{NC}-800$  and FeNC-800-M.

Sample	N content	graphitic N	pyridinic N	FeN	oxidized N	pyrrolic N
$\text{Fe}_3\text{C}/\text{NC}-800$	7.8%	36.5%	33.8%	14.5%	5.9%	9.3%
FeNC-800-M	4.5%	41.0%	31.4%	9.1	14.5%	13.1%

Table S2. Comparison of ORR catalytic performances in alkaline solution between  $\text{Fe}_3\text{C}/\text{NC}-800$  and other non-precious metal-based catalysts reported previously.

Catalyst	Onset potential	Half-wave potential	Mass loading	Ref.
	(V vs. RHE)	(V vs. RHE)	( $\mu\text{g cm}^{-2}$ )	
$\text{Fe}_3\text{C}/\text{NC}-800$	1.0	0.85	150	This work
NCNT/CoO-NiO-NiCo	1.0	0.83	210	1
D-AC@2Mn–4Co	0.88	0.80	160	2
GNPCSSs-800	0.957	0.82	200	3
Fe–N/C–800	0.92	0.81	100	4
NCNT/Ni–NiMn <sub>2</sub> O <sub>4</sub>		0.71	210	5
Co@Co <sub>3</sub> O <sub>4</sub> @C-CM	0.93	0.81	350	6
$\text{Fe}_1/\text{N}$ , S-PC	1.0	0.90	510	7
NC-900	0.83	0.68	100	8
Fe-N-C/rGO	0.94	0.81	3939	9
FePhen@MOF-ArNH <sub>3</sub>	1.03	0.86	3000	10
S–Fe/N/C	0.91	0.80	160	11
Fe-NCB-900	–	0.8	4000	12

Fe@C-NG/NCNTs	0.93	0.84	240	13
N-Fe/G(100)-900	0.89	0.81	50	14
Fe <sub>3</sub> C/C-800	1.05	0.83	600	15
Fe-N <sub>2</sub> -800	-0.077 V (vs. SCE)	-0.25 V (vs. SCE),	313	16
Fe <sub>3</sub> O <sub>4</sub> /FeNSG-3	0.95	0.81	200	17
Co@CoO@NC/C	0.92	0.81	420	18
CNPs	1.03	0.85	385	19
Fe-BC-800	0.94	0.80	420	20

Table S3. Comparison of ORR catalytic performances in acid media between Fe<sub>3</sub>C/NC-800 and other non-precious metal-based catalysts reported previously.

Catalyst	Onset potential (V vs. RHE)	Half-wave potential (V vs. RHE)	Mass loading ( $\mu\text{g cm}^{-2}$ )	Ref.
FeNC-800	0.88	0.7	150	This work
Fe <sub>3</sub> C/C-700	0.9	0.73	600	15
Fe-N-HCMS	0.81	0.6	1199	21
Fe <sub>3</sub> O <sub>4</sub> /FeNSG-3	0.75	/	200	17
CPANIFe-NaCl	0.91	0.74	600	22
PANI-Fe	0.85	/	600	23
Fe-N/C-800	0.8	0.68	100	24
pPMF-800	0.89	0.71	1200	25
Fe <sub>3</sub> C/NG-800	0.92	0.77	400	26

NH <sub>3</sub> -Fe <sub>0.25</sub> -N/C-900	0.94	0.68	125	27
FeNC-700	0.8	/	100	28
NH <sub>3</sub> -Fe <sub>0.25</sub> -N/C-900	0.94	0.71	400	27
H-Fe@N-C/RGO	0.89	0.67	315	29
N-Fe/G (60)-900-S	0.83	0.72	500	14
FeCo-PANI-TPP-NH <sub>3</sub>	0.85	0.73	2550	30
Fe-g-C <sub>3</sub> N <sub>4</sub> @C		0.75	600	31
PpPD-Fe-C	0.83	0.72	200	32
Fe-N-GC-900	/	0.74	600	33
N, P-CGHNs	0.9	0.68	600	34
Fe-N/MPC2	0.82	0.7	637	35
(Fe <sub>1-x</sub> S/N, S-MCNS) <sub>0.2</sub>	0.81	0.73	400	36
N/Fe-CG	0.93	0.73	170	37
Fe-N/C	0.8	0.55	270	38

### 3. Reference

- [1] X. Liu, M. Park, M. G. Kim, S. Gupta, G. Wu and J. Cho, *Angew. Chem. Int. Ed.*, **2015**, 54, 9654-9658.
- [2] X. Yan, Y. Jia, J. Chen, Z. Zhu and X. Yao, *Adv. Mater.*, **2016**, 28, 8771-8778.
- [3] H.-x. Zhong, J. Wang, Y.-w. Zhang, W.-l. Xu, W. Xing, D. Xu, Y.-f. Zhang and X.-b. Zhang, *Angew. Chem. Int. Ed.*, **2014**, 53, 14235-14239.
- [4] L. Lin, Q. Zhu and A. W. Xu, *J. Am. Chem. Soc.*, **2014**, 136, 11027-11033.
- [5] Q. Qin, L. Chen, T. Wei, Y. Wang and X. Liu, *Catal. Sci. Technol.*, **2019**, 9, 1595-1601.
- [6] W. Xia, R. Zou, L. An, D. Xia and S. Guo, *Energy Environ. Sci.*, **2015**, 8, 568-576.

- [7] K. Wu, X. Chen, S. Liu, Y. Pan, W.-C. Cheong, W. Zhu, X. Cao, R. Shen, W. Chen, J. Luo, W. Yan, L. Zheng, Z. Chen, D. Wang, Q. Peng, C. Chen and Y. Li, *Nano Res.*, **2018**, 11, 6260-6269.
- [8] A. Ajaz, N. Fujiwara and Q. Xu, *J. Am. Chem. Soc.*, **2014**, 136, 6790-6793.
- [9] C. Zhang, J. Liu, Y. Ye, Z. Aslam, R. Brydson and C. Liang, *ACS Appl. Mater. Interfaces*, **2018**, 10, 2423-2429.
- [10] K. Strickland, E. Miner, Q. Jia, U. Tylus, N. Ramaswamy, W. Liang, M. T. Sougrati, F. Jaouen and S. Mukerjee, *Nat. Commun.*, **2015**, 6, 7343.
- [11] K. Hu, L. Tao, D. Liu, J. Huo and S. Wang, *ACS Appl. Mater. Interfaces*, **2016**, 8, 19379-19385.
- [12] A. Serov, K. Artyushkova, E. Niangar, C. Wang, N. Dale, F. Jaouen, M.-T. Sougrati, Q. Jia, S. Mukerjee and P. Atanassov, *Nano Energy*, **2015**, 16, 293-300.
- [13] Q. Wang, Y. Lei, Z. Chen, N. Wu, Y. Wang, B. Wang and Y. Wang, *J. Mater. Chem. A*, **2018**, 6, 516-526.
- [14] Q. Lai, Q. Gao, Q. Su, Y. Liang, Y. Wang and Z. Yang, *Nanoscale*, **2015**, 7, 14707-14714.
- [15] Y. Hu, J. O. Jensen, W. Zhang, L. N. Cleemann, W. Xing, N. J. Bjerrum and Q. Li, *Angew. Chem. Int. Ed.*, **2014**, 53, 3675-3679.
- [16] D. Guo, S. Han, J. Wang and Y. Zhu, *Appl. Surf. Sci.*, **2018**, 434, 1266-1273.
- [17] Y. Li, Y. Zhou, C. Zhu, Y. H. Hu, S. Gao, Q. Liu, X. Cheng, L. Zhang, J. Yang and Y. Lin, *Catal. Sci. Technol.*, **2018**, 8, 5325-5333.
- [18] Z. Wu, J. Wang, L. Han, R. Lin, H. Liu, H. L. Xin and D. Wang, *Nanoscale*, **2016**, 8, 4681-4687.
- [19] S. Zhao, H. Yin, L. Du, L. He, K. Zhao, L. Chang, G. Yin, H. Zhao, S. Liu and Z. Tang, *ACS Nano*, **2014**, 8, 12660-12668.
- [20] X. Ma, Z. Lei, W. Feng, Y. Ye and C. Feng, *Carbon*, **2017**, 123, 481-491.
- [21] M. Zhou, C. Yang and K.-Y. Chan, *Adv. Energy Mater.*, **2014**, 4, 1400840.
- [22] W. Ding, L. Li, K. Xiong, Y. Wang, W. Li, Y. Nie, S. Chen, X. Qi and Z. Wei, *J. Am. Chem. Soc.*, **2015**, 137, 5414-5420.
- [23] H.-W. Liang, W. Wei, Z.-S. Wu, X. Feng and K. Muellen, *J. Am. Chem. Soc.*, **2013**, 135, 16002-16005.
- [24] L. Lin, Q. Zhu and A.-W. Xu, *J. Am. Chem. Soc.*, **2014**, 136, 11027-11033.
- [25] W. Yang, X. Yue, X. Liu, L. Chen, J. Jia and S. Guo, *Nanoscale*, **2016**, 8, 959-964.
- [26] M. Xiao, J. Zhu, L. Feng, C. Liu and W. Xing, *Adv. Mater.*, **2015**, 27, 2521-2527.
- [27] H. Tan, Y. Li, X. Jiang, J. Tang, Z. Wang, H. Qian, P. Mei, V. Malgras, Y. Bando and Y. Yamauchi, *Nano Energy*, **2017**, 36, 286-294.
- [28] T. Palanisvam, B. P. Biswal, R. Banerjee and S. Kurungot, *Chem. Eur. J.*, **2013**, 19, 9335-9342.
- [29] J. Wang, G. Wang, S. Miao, J. Li and X. Bao, *Faraday Discuss.*, **2014**, 176, 135-151.
- [30] Q. Zhang, J. Wang, P. Yu, F. Song, X. Yin, R. Chen, H. Nie, X. Zhang and W. Yang, *Carbon*, **2018**, 132, 85-94.
- [31] M.-Q. Wang, W.-H. Yang, H.-H. Wang, C. Chen, Z.-Y. Zhou and S.-G. Sun, *ACS Catal.*, **2014**, 4, 3928-3936.
- [32] Z. Xiang, Y. Xue, D. Cao, L. Huang, J.-F. Chen and L. Dai, *Angew. Chem. Int. Ed.*, **2014**, 53, 2433-2437.
- [33] A. Kong, X. Zhu, Z. Han, Y. Yu, Y. Zhang, B. Dong and Y. Shan, *ACS Catal.*, **2014**, 4, 1793-1800.
- [34] J. Yang, H. Sun, H. Liang, H. Ji, L. Song, C. Gao and H. Xu, *Adv. Mater.*, **2016**, 28, 4606-4613.
- [35] L. Osmieri, R. Escudero-Cid, M. Armandi, A. H. A. Monteverde Videla, J. L. Garcia Fierro, P. Ocon and S. Specchia, *Appl. Catal., B*, **2017**, 205, 637-653.
- [36] J. Xiao, Y. Xia, C. Hu, J. Xi and S. Wang, *J. Mater. Chem. A*, **2017**, 5, 11114-11123.
- [37] B. Li, S. P. Sasikala, D. H. Kim, J. Bak, I.-D. Kim, E. Cho and S. O. Kim, *Nano Energy*, **2019**, 56, 524-530.
- [38] D. Malko and A. Kucernak, *Electrochim. Commun.*, **2017**, 83, 67-71.